ISBN: 978-3-95450-261-5 ISSN: 2673-7000 doi: 10.18429/JACoW-NAPAC2025-MOXP02

APS UPGRADE: COMMISSIONING THE WORLD'S FIRST LIGHT SOURCE BASED ON SWAP-OUT INJECTION*

V. Sajaev†, M. Borland, J. Calvey, J. Dooling, L. Emery, K. Harkay, N. Kuklev, O. Mohsen, Y. Sun, N. Arnold, T. Berenc, A. Brill, H. Bui, J. Carwardine, W. Cheng, T. Fors, M. Kelly, R. Lindberg, G. Shen, M. Smith, F. Rafael, H. Shang, R. Soliday, U. Wienands, B. Yang
Argonne National Laboratory, Lemont, IL, USA

Abstract

The Advanced Photon Source (APS) has recently completed a major upgrade, replacing its 25-year-old storage ring with a cutting-edge hybrid seven-bend achromat lattice enhanced by six additional reverse bends. The new design achieves a natural emittance of 42 pm-rad, enabling the production of X-rays up to 500 times brighter than those generated by the original APS. A key innovation of the upgrade is the implementation of a swap-out injection scheme, which replaces entire depleted bunches instead of performing traditional top-up injection. This approach enables on-axis injection to accommodate for the reduced dynamic aperture resulting from strong focusing. This paper outlines the commissioning process, shares initial operating experience with swap-out injection, and presents performance data for new systems such as the bunch-lengthening cavity.

INTRODUCTION

The Advanced Photon Source (APS) recently completed a major upgrade [1], replacing its original double-bend achromat-based [2] storage ring [3] with a hybrid seven-bend achromat lattice, similar to the one implemented earlier at ESRF-EBS [4]. To further reduce the natural emittance, the APS Upgrade (APS-U) lattice incorporates six reverse bends in addition to the seven main bending magnets [5, 6]. The new design also utilizes swap-out injection [7, 8], which enables operation with a smaller dynamic aperture – a key factor in achieving ultra-low emittance.

As part of the upgrade, the electron beam energy was reduced from 7 GeV to 6 GeV, necessitating modifications of all insertion devices. The project also included the construction of seven entirely new beamlines, as well as significant modifications to most of the remaining beamlines to accommodate for the new source characteristics. Although the injector complex – comprising a 450-MeV linear accelerator [9], the Particle Accumulator Ring (PAR) [10], and the booster [11] – was not part of the official APS-U scope, it underwent targeted refurbishment in parallel to enhance reliability and operational performance.

APS operations were halted on April 24, 2023, to begin the storage ring replacement and injector maintenance. The linac was restarted in September 2023, followed by the PAR in October, and the booster in Febuary 2024 [12, 13]. Assembly of the upgraded storage ring was completed on February 15, and, after extensive tests without beam, the commissioning approval was granted on April 10, 2024. In this paper, we present an overview of the commissioning process and summarize the performance of the new storage ring.

APS-U COMMISSIONING

BTS Commissioning

Commissioning officially started when the beam was extracted from the Booster into the Booster-to-Storage Ring (BTS) transfer line. The Booster-to-Storage Ring (BTS) transfer line is divided into two sections by the wall separating the booster and storage ring tunnels. The booster-side section of the BTS remained unchanged, while the storage ring (SR) section was completely redesigned to accommodate the new SR geometry. A key feature of the redesigned BTS is the emittance exchange section, which consists of six skew quadrupoles configured to exchange the horizontal and vertical emittances of the beam extracted from the booster [14]. This exchange is necessary to match the injected beam to the narrow 2.8 mm horizontal gap between the outboard wall of the septum magnet and the inboard blade of the first injection kicker.

The original BTS section features a relatively large-aperture vacuum chamber and three one-plane stripline BPMs. In contrast, the new SR-side BTS section has a reduced aperture and is equipped with 11 two-plane button BPMs, providing improved diagnostics suited to the tighter aperture.

When the first beam was extracted from the booster, it successfully traversed the booster-side section of the BTS but was lost between the last BPM in the large-aperture booster section and the first BPM in the redesigned, smaller-aperture storage ring (SR) section. Trajectory correction program failed to advance the beam beyond that point using corrector magnets only. Subsequently, a transmission optimization routine that varied both corrector magnets and quadrupole strengths was able to push the beam farther along the BTS – nearly to its end – but still with significant losses, and no beam could be injected into the storage ring.

Further investigation revealed that the quadrupole changes made by the optimization routine, which improved beam transport past the initial loss point, were consistent with a scenario in which all five quadrupoles in the legacy (booster-side) section of the BTS were powered with reversed polarity. This hypothesis was confirmed by trajectory response measurements. The reversed polarity had a plausible explanation: the original APS was designed to operate with positrons,

* Work supported by the U.S. Department of Energy, Office of Science, Office of Basic Energy Sciences, under Contract No. DE-AC02-06CH11357.
† sajaev@anl.gov

ISBN: 978-3-95450-261-5 ISSN: 2673-7000 doi: 10.18429/JACoW-NAPAC2025-MOXP02

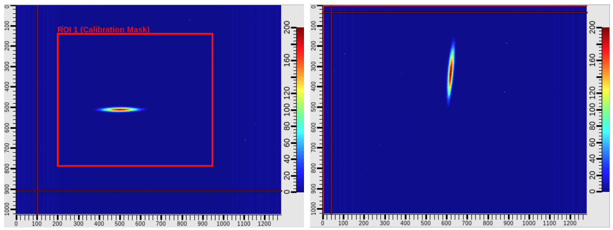

Figure 1: Beam image in the BTS transfer line before (left) adn after (right) the emittance exchange section.

but operated most of its lifetime with electrons. Switching between particle types was achieved by reversing magnet polarities at the power supplies. During APS-U construction, the magnets in this section were disconnected and later reconnected – but, unlike the newly installed storage ring magnets whose polarity was systematically verified, the legacy BTS quadrupoles were not rechecked. Tunnel inspection confirmed that all five quadrupoles in the booster-side BTS section had indeed been reconnected with reversed polarity. Once the polarity was corrected, the trajectory correction program was able to steer the beam into the storage ring without issue. Figure 1 shows the beam image in the BTS before and after the emittance exchange section.

Storing First Beam

After scanning the injection kicker timing to maximize beam transmission, the beam reached Sector 28, but with significant losses in the initial sectors. Optimization of the transfer line exit trajectory improved transmission, allowing 100% of the beam to reach Sector 13; however, full beam loss still occurred at Sector 28. Manual adjustment of harmonic orbit knobs enabled the beam to complete the first turn without losses, but it was lost early on the second turn.

First-turn trajectory correction reduced the trajectory deviation to within ±2 mm, which allowed the beam to circulate for up to five turns. Clear losses were localized near the septum magnet. Subsequent transmission optimization – including tuning of the BTS trajectory, BTS quadrupoles, storage ring tunes, septum, and injection kicker parameters – extended beam circulation to 15 turns. At this point, tunnel shielding verification began. This involved dumping first-turn beam at various locations while monitoring radiation levels outside the tunnel and lasted approximately 80 hours.

Upon completing shielding verification, efforts to store beam resumed. RF voltage was turned on, and the booster-to-storage-ring RF phase was set based on a phase scan that measured beam energy as a function of turn number. With RF on, transmission increased to 80 turns, although significant losses persisted near the injection point. After turning the sextupoles on, a Bayesian optimizer was employed to vary orbit bumps near the injection region, betatron tunes, RF frequency, and BTS correctors and quadrupoles. This process led to the first measurable stored beam – approximately 40 µA – with a lifetime of 4 seconds. However, the beam conditions were unstable, and the tunes had shifted significantly.

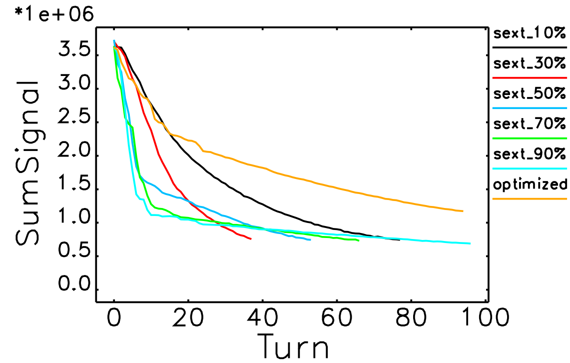

Figure 2: BPM sum signal showing beam transmission during sextupole ramp. The trajectory recording program used a no-beam threshold set to 20% of the initial beam intensity to avoid applying trajectory corrections based on weak signals. As a result, all curves in the plot are truncated at 0.7×10^{-6}.

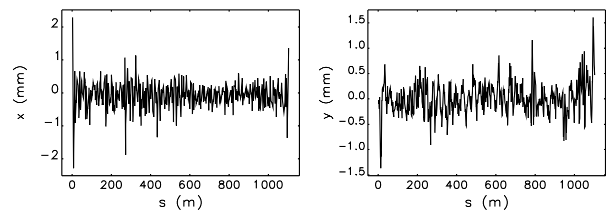

Figure 3: First measurement of the closed orbit.

A key outcome of the optimizer was the identification of a +2 mm horizontal orbit bump at the injection point, strongly suggesting the presence of a physical aperture limitation in that region. Based on this, all parameters – tunes, RF frequency, sextupoles, BTS settings, and correctors – were returned to their pre-optimization values, while the orbit bump discovered by the optimizer was retained. With these settings, a quasi-closed orbit correction and sextupole ramp were initiated. After just a few correction iterations, at 90% sextupole strength, 50 µA of stored beam was captured with a lifetime of 10 minutes, corresponding to an injection efficiency of 20%. The rapid beam capture was achieved by the automated trajectory correction but relied on the orbit bump at the septum location found by the Bayesian optimizer. Further optimization using orbit correctors raised injection efficiency to 70%.

Figure 2 shows the BPM sum signal during the sextupole ramp. Notably, as sextupole strength increased, beam transmission over 100 turns initially degraded before recovering as the sextupoles approached full strength – a behavior consistent with improved chromaticity correction. Figure 3 shows the closed orbit corresponding to the first stored beam, while Fig. 4 shows the horizontal orbit zoomed in at the injection point to show the orbit bump that was necessary to store the first beam.

Swap-Out Injection

Up until this moment, the commissioning was being done with a single bunch. In order to be able to run swap-out injection, operation of decoherence [15] and fan-out [16] kickers needed to be set up and verified. Decoherence kicker fires

ISBN: 978-3-95450-261-5 ISSN: 2673-7000 doi: 10.18429/JACoW-NAPAC2025-MOXP02

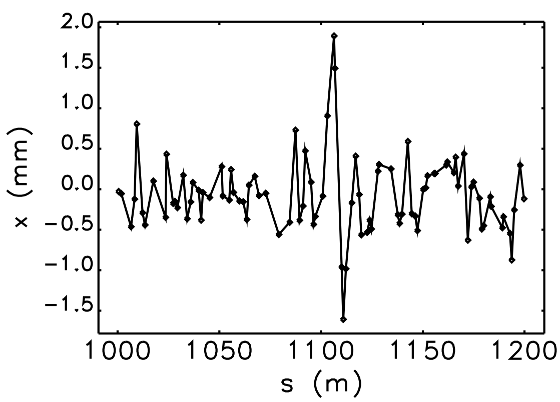

Figure 4: Horizontal orbit around the injection point, which is located at s=1104 m, showing large positive orbit required for injection.

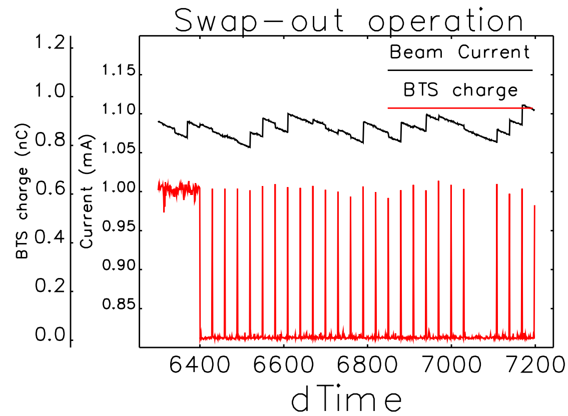

Figure 5: First multi-bunch swap-out with 12-bunch fill pattern. Beam current target is 1.1 mA, swap-out interval is 30 seconds, BTS charge is 0.6 nC.

250 turns before every swap-out injection to excite vertical oscillations of the bunch to be swapped out. This is done to protect the surface of the swap-out beam dump by increasing the beam size of that bunch to reduce its energy density. Fan-out kicker is activated during whole beam dumps to also to protect the surface of the whole beam dumps. The fan-out kicker has a half-sine waveform extending for the full turn, so that each stored bunch gets different vertical kick amplitude to spread out the bunches along the surface of the beam dumps.

After kicker setup and verifications were completed, the swap-out program was started. The program fills the requested fill pattern at 1 Hz, and then swaps out the weakest bunch at requested intervals. Figure 5 shows the first multi-bunch swap-out operation at the target of 1.1 mA with 30 seconds swap-out interval using BTS charge of 0.6 nC. Multi-bunch swap-out injection has been running since that moment.

Septum Failures

The APS-U injection septum magnet is a pulsed, single-turn, direct-drive magnet, similar in concept to the septa used in the original APS storage ring [17]. It delivers a peak field of 1.42 T over a straight magnetic length of 1.493 m, with a septum blade that tapers to 3 mm thickness at the downstream end to separate the high-field injected beam region from the field-free stored beam path.

Commissioning was interrupted twice due to failures of the storage ring injection septum. The first incident occurred after 23 days of operation (about one million pulses), when the 1-mm-thick copper main bus, carrying a peak current of 18 kA, ruptured at the location of a small unsupported gap in the bus structure. A spare septum was quickly modified to eliminate the unsupported gap, installed, and commissioning resumed. However, after another 22 days, the second septum developed a vacuum leak in the stored beam chamber, later traced to a manufacturing defect. By that time, the original septum had been repaired and was reinstalled.

During reinstallation of the repaired first septum, mechanical survey revealed the root cause of an unexpectedly large orbit bump required for injection. It was found that the stored beam vacuum chamber bowed outward inside the magnet, such that the inboard wall of the vacuum chamber touched the design closed orbit approximately 0.7 m from the downstream end of the magnet. The nominal design clearance between the chamber wall and the beam orbit is 3 mm. It was impossible to fix this aperture limitation in place. Because the downstream end of the septum is mechanically fixed at the injection point, the magnet was rotated by 0.7 mrad around this point to move the aperture constraint slightly away from the beam trajectory. This septum remains in operation while a new design is under development to meet the intended aperture specifications.

Optics Correction and Emittance Measurements

First optics measurement was performed very soon after storing the first beam. Orbit response matrix with 20 correctors per plane were used for the optics measurement [18, 19]. The measurement was performed with single bunch at 0.1 mA. The resulting beta functions are shown in Fig. 6. While emittances were not directly measured, model-based calculations [20] using `elegant` [21] predicted $\epsilon_x = 70$ pm and $\epsilon_y = 90$ pm. Lattice correction was not performed at this point due to expected poor orbit measurement accuracy at this low beam current.

After commissioning of multi-bunch operation, the lattice was remeasured and used as the basis for lattice correction. Several iterations of correction were applied over the following weeks of commissioning. Figure 7 shows the resulting lattice functions after correction.

Emittance of the electron beam was calculated from photon beam size and divergence measurements using undulator radiation [22]. The measurements were performed for low coupling (flat beam) and for full coupling (round beam) conditions. Table 1 gives the results. For these measurements, all insertion device gaps were open except for the device used for the measurements. The results match the simulations well and demonstrate that APS-U has reached its goal emittance.

ISBN: 978-3-95450-261-5 ISSN: 2673-7000 doi: 10.18429/JACoW-NAPAC2025-MOXP02

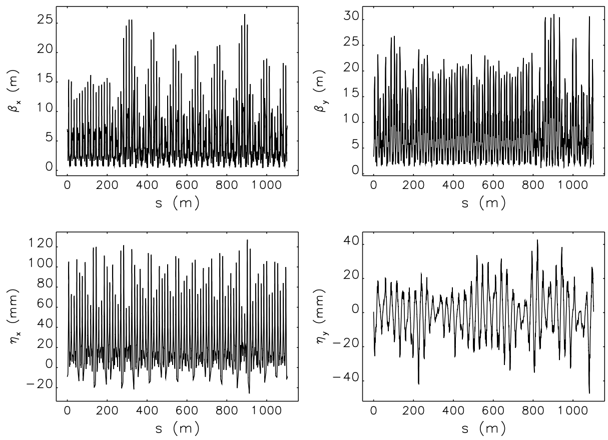

Figure 6: First lattice measurements right after storing first beam. Model is derived from response matrix measurements.

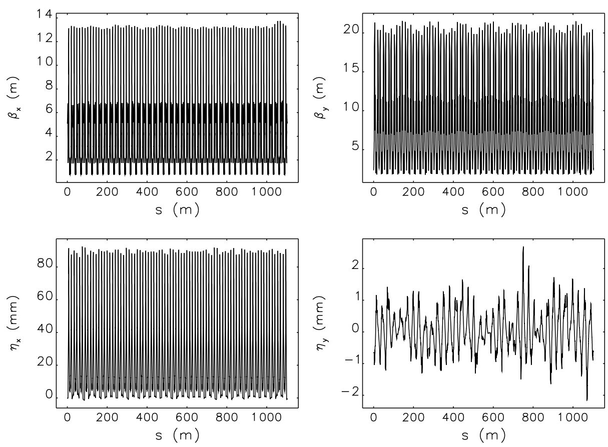

Figure 7: Lattice functions after several iterations of lattice correction.

Table 1: Emittance Measurement Results

	Horizontal	Vertical
	Full coupling	
Total source size (µm)	13.0	9.8
Total divergence (µrad)	4.9	5.6
Measured emittance (pm·rad)	28 ± 3	31 ± 2
Emittance from model (pm·rad)	31	31
	Low coupling	
Total source size (µm)	16.1	4.9
Total divergence (µrad)	5.2	4.5
Measured emittance (pm·rad)	44 ± 3	3.3 ± 2
Emittance from model (pm·rad)	44	2.9

Orbit Motion

The APS Upgrade project set an orbit stability requirement of 10% of the electron beam size. To meet this stringent specification, the original plan included development of an advanced fast orbit correction system with a 22 kHz update rate and a target correction bandwidth of 1 kHz [23]. However, during the course of the project, modeling indicated that the anticipated uncorrected orbit motion would likely remain within or close to specification even without fast feedback [24]. As a result, development of the fast orbit feedback system was deferred, and initial orbit correction was implemented using a slower workstation-based process operating at 1 Hz [25].

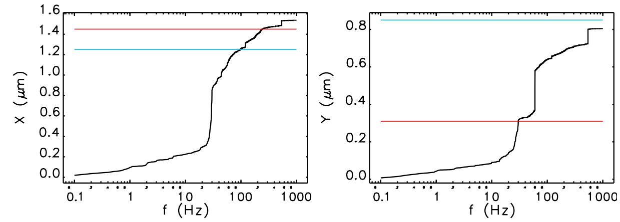

Figure 8: Rms orbit motion at ID location. Horizontal lines are orbit stability requirements, red line – low coupling, blue line – full coupling.

Soon after storing first beam, significant 1 Hz orbit motion was observed in the horizontal plane, with rms amplitude – including harmonics – approaching 4 µm, significantly exceeding the stability specification. Investigation revealed that the motion originated from M1 and M2 dipole power supplies responding to voltage sag on the AC line caused by the booster ramping power supplies. After internal power supply parameters were tuned, the 1 Hz motion was eliminated entirely. The next dominant disturbance in the horizontal plane was identified at 30 Hz, attributed to mechanical vibrations of the magnet girders. Figure 8 shows the measured rms orbit motion with requirement thresholds indicated, confirming that uncorrected orbit motion is close to specification.

The planned fast-orbit feedback system is under development. Meanwhile, a stop-gap system with a 50-Hz update rate was created using the same workstation-based tools [26], making use of the turn-by-turn BPM data acquisition system [27] to produce averaged waveforms for 240 correctors at the required rate. Although this cannot suppress the 30-Hz motion, it is effective in isolating beamlines from one another and provides for rapid response to beamline steering requests.

Bunch-Lengthening System (BLS)

Due to the small electron beam size in the APS-U storage ring, the expected Touschek lifetime is relatively short. To mitigate this, a new bunch-lengthening system [28] has been installed, featuring a single-cell passive superconducting cavity operating at the fourth harmonic (1408 MHz) of the main RF frequency [29]. This passive, beam-driven system increases the bunch length by a factor two to four, thereby reducing the charge density and enhancing the Touschek lifetime. The cavity operates at 2.1 K and has been successfully tested to provide a 1.1 MV voltage at a beam current of 200 mA. Figure 9 show the measurement of beam lifetime as a function of BLS voltage. In user operation with 200 mA, the BLS is currently operated at 1.1 MV.

Vacuum Conditioning

Before opening beamline shutters, vacuum conditioning is required to reduce outgassing, improve overall vacuum

ISBN: 978-3-95450-261-5 ISSN: 2673-7000 doi: 10.18429/JACoW-NAPAC2025-MOXP02

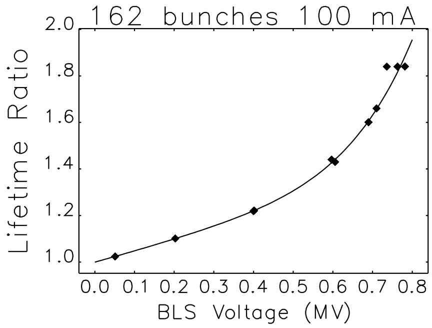

Figure 9: Lifetime as a function of BLS voltage measured at 100 mA with 162 bunches. Lifetime at zero voltage is 1.5 hours.

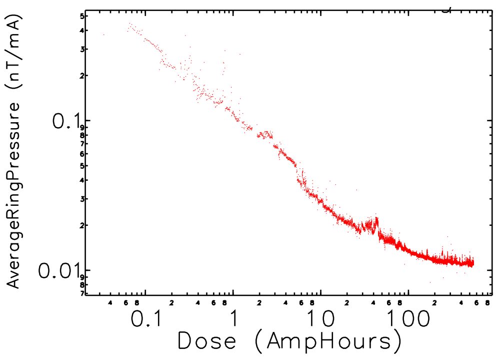

Figure 10: Average vacuum pressure in the storage ring as a function of accumulated dose.

levels, and suppress bremsstrahlung radiation. Vacuum conditioning shifts began immediately after the start of multi-bunch swap-out injection and were carried out during night-time hours by machine operators, while storage ring and beamline commissioning activities proceeded during the day.

Figure 10 shows the average pressure in the storage ring as a function of accumulated dose. In computing the average pressure, data from four sectors – representing 10% of the ring – were excluded due to known vacuum leaks and anomalous pressure readings from certain sensors. These leaks have not yet been repaired due to other competing priorities. The vacuum system was designed with the goal of achieving an average pressure of 0.01 nTorr/mA after accumulating 1000 Amp-hours of beam dose. Notably, the measured average pressure approached this target value after just 300 Amp-hours, indicating effective conditioning performance ahead of schedule.

Beam Current Ramp

Machine commissioning was carried out in two main phases: an initial dedicated machine commissioning period, followed by a phase of parallel machine and beamline commissioning. The first phase spanned from April 10 to June 17, during which beam current was gradually increased in parallel with core machine setup and performance verification activities. The second phase, from June 17 to August 12, involved shared use of beam time among machine commissioning, beamline commissioning, and vacuum conditioning.

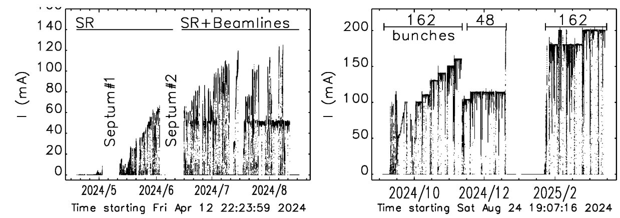

Figure 11: Beam current ramp during commissioning (left) and during user operation (right).

During this period, vacuum conditioning shifts – typically conducted overnight – were also used to continue ramping up the beam current. The progression of beam current during commissioning is shown in Fig. 11 (left).

Full 24-hour user operations commenced in September 2024, with two primary operating modes: multi-bunch mode with 162 bunches and timing mode with 48 bunches. Due to current injector limitations, timing mode operation is restricted to a maximum beam current of 140 mA. The beam current ramp during user operation is shown in Fig. 11 (right). The target beam current of 200 mA was successfully reached in March 2025.

CONCLUSION

APS-U storage ring is the first synchrotron light source that utilizes swap-out injection to allow for operation with small dynamic aperture. This allowed to design the lattice with natural emittance of 42 pm-rad, which was confirmed in measurements during commissioning. Dedicated storage ring commissioning took just over two months and allowed to reach 25 mA to enable beginning of beamline commissioning in parallel with storage ring work. Five months after commissioning started, the round-the-clock user operation started with 100 mA beam current. Over the next 6 months, the beam current was ramped to the design value of 200 mA.

REFERENCES

[1] M. Borland *et al.*, "The upgrade of the Advanced Photon Source", pp. 2872–2877, 2018. doi:10.18429/JACoW-IPAC2018-THXGBD1

[2] R. Chasman, G. K. Green, and E. M. Rowe, "Preliminary design of a dedicated synchrotron radiation facility", in *Proc. PAC'75*, Washington D.C., USA, Mar. 1975, pp. 1765–1768.

[3] G. Decker, "Performance of the Advanced Photon Source", in *Proc. PAC'97*, Vancouver, B.C., Canada, May 1997, paper 4B001, pp. 698–702.

[4] J. C. Biasci *et al.*, "A low-emittance lattice for the ESRF", *Synchrotron Radiat. News*, vol. 27, no. 6, pp. 8–12, 2014. doi:10.1080/08940886.2014.970931

[5] J. Delahaye and J. P. Potier, "Reverse bending magnets in a combined-function lattice for the CLIC damping ring", in *Proc. PAC'89*, Chicago, IL, USA, Mar. 1989, pp. 1611–1613.

[6] A. Streun, "The anti-bend cell for ultralow emittance storage ring lattices", *Nucl. Instrum. Methods Phys. Res. A*, vol. 737, pp. 148–154, 2014. doi:10.1016/j.nima.2013.11.064

[7] L. Emery and M. Borland, "Possible long-term improvements to the Advanced Photon Source", in *Proc. PAC'03*, Portland,

ISBN: 978-3-95450-261-5 ISSN: 2673-7000 doi: 10.18429/JACoW-NAPAC2025-MOXP02

Oregon, USA, May 2003, paper TOPA014, pp. 256–258. https://jacow.org/p03/papers/TOPA014.pdf

[8] R. Abela, W. Joho, P. Marchand, S. V. Milton, and L. Z. Rivkin, "Design considerations for a Swiss Light Source (SLS)", in *Proc. EPAC'92*, Berlin, Germany, Mar. 1992, pp. 486–489.

[9] M. White, "Construction, commissioning and operational experience of the Advanced Photon Source (APS) linear accelerator", in *Proc. LINAC'96*, Ottawa, Ontario, Canada, Aug. 1992, paper TU301, pp. 315–322. https://jacow.org/l96/papers/TU301.pdf

[10] M. Borland, "Construction and commissioning of the positron accumulator ring for the APS", *Nucl. Instrum. Methods Phys. Res. B*, vol. 99, p. 271, 1999. doi:10.1016/0168-583X(95)00213-8

[11] S. Milton, "The APS booster synchrotron: commissioning and operational experience", in *Proc. PAC'95*, Dallas, Texas, USA, May 1995, pp. 594–596.

[12] K. Harkay *et al.*, "Particle accumulator ring restart and readiness for Advanced Photon Source Upgrade commissioning", in *Proc. IPAC'24*, Nashville, TN, USA, May 2024, pp. 1228–1231. doi:10.18429/JACoW-IPAC2024-TUPG06

[13] J. Calvey *et al.*, "APS upgrade booster commissioning", in *Proc. IPAC'24*, Nashville, TN, USA, May 2024, pp. 1232–1235. doi:10.18429/JACoW-IPAC2024-TUPG07

[14] P. Kuske and F. Kramer, "Transverse emittance exchange for improved injection efficiency", in *Proc. IPAC'16*, Busan, Korea, Aug.–May 2016, pp. 2028–2031. doi:10.18429/JACoW-IPAC2016-WEOAA01

[15] M. Borland, J. C. Dooling, R. R. Lindberg, V. Sajaev, and A. Xiao, "Using Decoherence to Prevent Damage to the Swap-Out Dump for the APS Upgrade", in *Proc. IPAC'18*, Vancouver, Canada, Apr.-May 2018, pp. 1494–1497. doi:10.18429/JACoW-IPAC2018-TUPMK004

[16] J. C. Dooling *et al.*, "Measuring the effects of fast beam loss on the APS-U collimators", presented at IBIC'25, Liverpool, UK, Aug. 2025, paper MOPMO42, unpublished.

[17] S. Sheynin and others, "The APS direct-drive pulsed septum magnets", pp. 1355–1357, 1996.

[18] J. Safranek, "Experimental determination of storage ring optics using orbit response measurements", *Nucl. Instrum. Methods Phys. Res. A*, vol. 388, 1997. doi:10.1016/S0168-9002(97)00309-4

[19] V. Sajaev and L. Emery, "Determination and Correction of the Linear Lattice of the APS Storage Ring", in *Proc. EPAC'02*, Paris, France, Jun. 2002, paper TUPRI001, pp. 742–744. https://jacow.org/e02/papers/TUPRI001.pdf

[20] K. Ohmi, K. Hirata, and K. Oide, "From the beam-envelope matrix to synchrotron-radiation integrals", *Phys. Rev. E*, vol. 49, no. 1, pp. 751–765, Jan. 1994. doi:10.1103/PhysRevE.49.751

[21] M. Borland, "Elegant: a flexible SDDS-compliant code for accelerator simulation", Advanced Photon Source, Rep. LS-287, Sep. 2000. http://www.aps.anl.gov/Science/Publications/lsnotes/ls287.pdf

[22] X. Shi *et al.*, *J. Synchrotron Radiat.*, to be published.

[23] N. Sereno *et al.*, "First beam tests of the APS MBA upgrade orbit feedback controller", in *Proc. IBIC'16*, Barcelona, Spain, Sep. 2016, pp. 39–42. doi:10.18429/JACoW-IBIC2016-MOPG06

[24] V. Sajaev, Z. Liu, J. Nudell, and C. Preissner, "Calculation of expected orbit motion due to girder resonant vibration at the APS upgrade", in *Proc. IPAC'18*, Vancouver, Canada, Apr.–May 2018, pp. 1269–1271. doi:10.18429/JACoW-IPAC2018-TUPMF011

[25] L. Emery and M. Borland, "Advances in orbit drift correction in the Advanced Photon Source storage ring", in *Proc. PAC'97*, Vancouver, Canada, May 1997, paper 3V001, pp. 742–744.

[26] M. Borland, "Applications Toolkit for Accelerator Control and Analysis", in *Proc. PAC'97*, Vancouver, Canada, May 1997, paper 6P020, pp. 2487–2489.

[27] S. Veseli *et al.*, "Data Acquisition System for the APS Upgrade", in *Proc. ICALEPCS'19*, Brooklyn, New York City, NY, USA, Oct. 2019, p. 842. doi:10.18429/JACoW-ICALEPCS2019-TUDPP02

[28] J. Byrd and M. Georgsson, "Lifetime increase using passive harmonic cavities in synchrotron light sources", *Phys. Rev. Spec. Top. Accel.Accel. Beams*, vol. 4, no. 3, p. 030701, Mar. 2001. doi:10.1103/PhysRevSTAB.4.030701

[29] M. Kelly *et al.*, "Installation and commisisoning of the APS-U bunch lengthening system", in *Proc. IPAC'24*, Nashville, TN, USA, May 2024, pp. 2713–2716. doi:10.18429/JACoW-IPAC2024-WEPS10